

04

## Generation of narrowly focused radiation of neutrons in a plasma-focus discharge — discovery and prospects of research

© V.E. Ablesimov, A.G. Malkin, O.Yu. Pasharina

Russian Federal Nuclear Center, All-Russia Research Institute of Experimental Physics, Sarov, Russia  
e-mail: ablesimov\_v@mail.ru

Received June 10, 2022

Revised July 27, 2022

Accepted July 27, 2022

Analysis of the measurement results by scintillation detectors of the time dependence of the output of DD neutrons in a plasma-focus discharge indicates the generation of a narrowly directed neutron beam in the discharge. The quantitative characteristics of a narrowly directed neutron beam are estimated — the output of neutrons in the beam, the duration of generation, and the angular divergence of the beam. To estimate the beam parameters, the Monte Carlo simulation of the features of the time dependence of the signal of the scintillation detector in the conditions of a closed space in which the measurements were carried out was carried out.

**Keywords:** plasma focus, generation of DD neutrons, scintillation detectors, time-of-flight method, Monte Carlo method.

DOI: 10.21883/TP.2022.11.55172.153-22

### Introduction

Measuring the neutron yield from plasma focus devices is one of the most informative methods for diagnosing a deuterium-filled plasma focus (PF), as it provides clear evidence for the nature of the fusion reaction mechanism. The neutron yield value is the most important characteristic of the plasma chamber also from the point of view of applications. The study of neutron generation processes in PF devices is both of practical importance and contributes to a deeper understanding of the fusion reaction mechanisms in these devices.

Years of research have shown that neutron generation in PFs is due to two main mechanisms — fusion and acceleration („beam–target“ model), with varying relative contributions depending on the design of the particular device and its mode of operation. Determining the relative contribution of both mechanisms to the total generation of neutron radiation is very difficult both theoretically and experimentally. The question of the identity of the time parameters of neutron generation for these mechanisms is poorly investigated.

Anisotropy of the yield and energy of the generated neutrons is associated with the accelerator mechanism of fusion. The value of neutron fluence anisotropy is usually less than 2 (the ratio of neutron output along the plasma chamber axis to the output perpendicular to the axis). In some experiments [1–3] an abnormally high degree of neutron fluence anisotropy is observed — from 3.3 to 6. The neutron energy in the axial direction usually does not exceed 2.9 MeV, in the direction perpendicular to the axis is 2.5–2.6 MeV [4,5]. An extensive review and bibliography of works on the study of neutron generation and fluxes of charged particles in plasma-focused devices is given in [6].

In a study of the characteristics of the plasma focus chamber of the Meisser type described in work [7], the initial pressure of deuterium in the discharge chamber was 8 Torr (1 kPa). The capacitor battery was charged to a voltage of 38 kV. The discharge current reached a maximum value of 1.2 MA about three microseconds after the arresters were triggered. The energy in the discharge is estimated by the value  $\sim 45$  kJ. Parameters of the generated radiation were measured with scintillation detectors (SD), measurements of the time dependence of the neutron yield from the device by the time-of-flight method were carried out. We used SSDI-8 [8] type SDs with organic plastic scintillator (polystyrene + *p*-terphenyl) mounted at distances 6 and 9 m from the PF.

The experimental hall is  $18 \times 12$  m in size and 7.5 m high. The camera was positioned vertically, with the upper end facing the ceiling of the hall. The source of radiation (PF) was placed at a height of 2.06 m from the floor. The minimum distance to the nearest wall was 4.5 m, to the concrete ceiling —  $\sim 5.5$  m. The direction from the source to the detectors was  $\sim 80^\circ$  to the camera axis. The layout of the equipment (PF-chamber, CB-capacitor battery, SD) in the hall is shown in Fig. 1.

The result of SD measurements is the time dependence (oscillogram) of the current induced in the detector by the pulse of radiation acting on it. Oscillograms of the detector signal allow to determine the time characteristics of the radiation pulse. The integral neutron yield is determined by the area of the neutron component of the detector signal, taking into account the contribution of scattered radiation. The oscillogram of the SD signal in the experiments under consideration has a complex structure, corresponding to the variety of emission generation processes in the

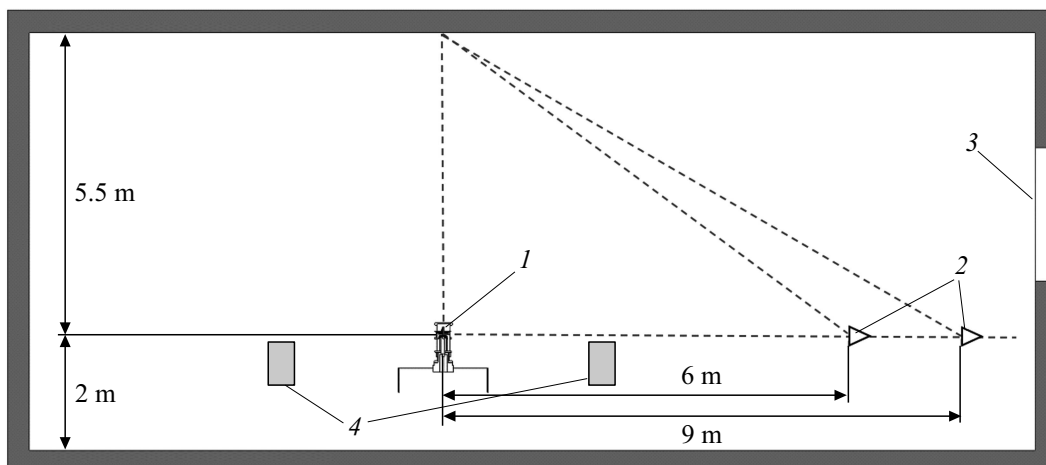


**Figure 1.** Schematic of the arrangement of the PF-chamber and SD-detectors in the experimental room: 1 — PF-chamber, 2 — SD-detectors, 3 — window, 4 — capacitor batteries.

plasma chamber and the contribution of scattered radiation components to the detector signal.

### 1. Peculiarities of the time dependence of the SD signal and their evaluation

The characteristic shape of the time dependence of the signals of the detectors placed at distances 6 and 9 m from the PF is shown in Fig. 2. The beginning of the timeline — the moment of radiation generation. Vertical axis — signal amplitude in volts.

When analyzing the results, a peculiarity of the time dependence of the SD signal was noted, which consists in the fact that in a number of discharges (shot) after the main peak of neutron emission  $n$ , corresponding to the time of neutron flyby with energy about 2.5–2.7 MeV distance to the detectors (6 and 9 m) — between 500–550 ns for distance 6 m and 620–700 ns for 9 m — there is more or less pronounced  $n_{scat}$  peak with characteristic width at half-height  $\sim 50$  ns, superimposed on the „tail“ of the main pulse. The first peak ( $\gamma + X$ ) — a superposition of hard X-ray radiation ( $X$ ), not related to neutron generation, and gamma radiation ( $\gamma$ ) from inelastic interaction processes of neutrons with PF-chamber materials.

In some discharges, the  $n_{scat}$  peak of scattered neutrons may be almost indistinguishable (or absent) in the signal structure. Such a case is illustrated by the experimental oscillogram in Fig. 3.

The analysis of the time dependence of the discharge current and its derivative (the presence of only one „feature“ on the oscillograms) excludes the possibility of explaining the observed phenomenon by repeated pinching. This applies to all discharges, the characteristics of which are shown in the table below. The indicated current dependences are almost identical for both discharges with and without the  $n_{scat}$  peak.

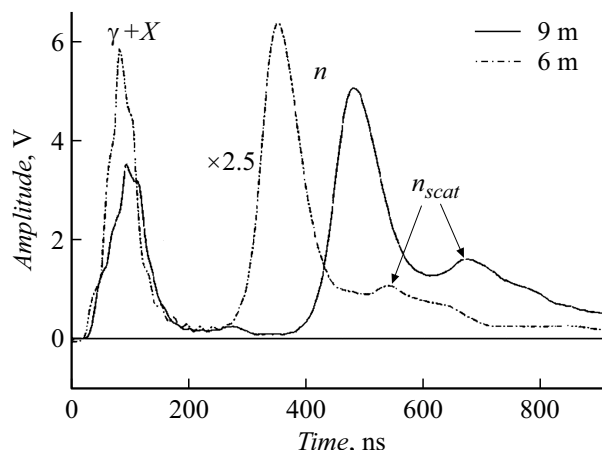


**Figure 2.** Characteristic features of scintillation detector signal in the presence of peak  $n_{scat}$ .

The hypothesis of scattering of a narrowly focused neutron beam exiting along the axis of the PF-chamber in a limited region of the ceiling of the experimental hall was considered as a possible reason for the appearance of the  $n_{scat}$  peak in the time dependence of the SD signal. The proposed hypothesis was justified by Monte Carlo simulation of the detector signal using the C-007 method described in [9]. A preliminary test of the hypothesis of generation of a narrow-directional beam of DD neutrons in the experiments was carried out in work [10]. Verification confirmed that this hypothesis explains the observed in the experiment peculiarities of the time dependence of the SD signal, corresponding to the escape of neutrons from the plasma-focused chamber.

To assess the quantitative characteristics of the neutron peaks recorded on the oscillograms of SD signals during measurements, we processed a series of experimental oscillograms for the distance 9 m between the source and

Parameters of neutron pulses

№ item	№ discharge	$t_{dir}$ , ns	$t_{scat}$ , ns	$t_{1/2,dir}$ , ns	$t_{1/2,scat}$ , ns	$S_{dir}$ , V·s	$S_{scat}$ , V·s	$t_{c,dir}$ , ns	$t_{c,scat}$ , ns	$S_{dir}/S_{scat}$	AC, counts/(100 s)
1	20	401	630	106	71	5.72E-07	4.48E-08	491	689	13	8765
2	44	403	621	75	53	3.98E-07	2.00E-08	476	666	20	9182
3	41	404	627	99	49	3.35E-07	6.96E-09	496	663	48	6708
4	36	402	660	90	46	1.78E-07	9.96E-09	482	697	18	4091
5	64	398	602	81	62	4.37E-07	4.14E-08	464	646	11	7498
6	57	402		72		3.23E-07		468			6618
7	63	398		68		3.60E-07		463			7115

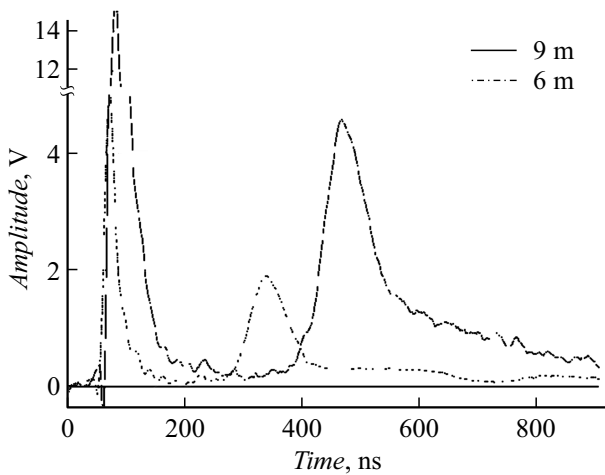


Figure 3. Time dependence of detector signals. There is no peak  $n_{scat}$ .

the detector, similar to those presented in Fig. 2, 3. The leading edge of the direct and scattered neutron peaks was approximated by a Gaussian, for which the full width at half maximum (FWHM) and the area were determined. It is clear that the shape of the trailing front of neutron peaks is significantly distorted by lower-energy neutrons and scattered radiation.

The arrival times of direct and scattered neutrons with maximum energy ( $t_{dir}$  and  $t_{scat}$ ) on the detector were determined as the moment when the tangent to the leading edge of the neutron peak crosses the „substrate“ — the background signal level due to scattered radiation.

Parameters (characteristics) of neutron peaks processed in the specified way are given in the table.

In tables  $t_{dir}$  and  $t_{scat}$  — arrival times to the detector of neutrons with maximum energy (direct and scattered from the hall ceiling),  $t_{1/2,dir}$  and  $t_{1/2,scat}$  — width at half-height of the approximating Gaussian,  $S_{dir}$  and  $S_{scat}$  — the area of the approximating Gaussian in the coordinates of the experimental oscillogram (volt-second),  $t_{c,dir}$  and  $t_{c,scat}$  — the time coordinate of the peak of direct and scattered neutrons respectively.

The last two rows of the table show the pulse parameters for discharges in which no scattered radiation peak is observed.

According to the results of processing the oscillograms presented in the table, we can conclude the following.

The areas of the direct and scattered peaks do not correlate with each other, which means that the corresponding processes of neutron generation, responsible for the manifestation of these peaks, are independent.

The neutron energy corresponding to the beginning of the leading edge of the direct peak is  $\sim 2.6$  MeV. The peak width (FWHM), determined from the leading edge, is 70–90 ns. This value is individual for each peak and is the upper value of the neutron generation duration — the pulse duration in the oscillogram increases due to blurring by neutrons of lower energies, in particular neutrons of a possible thermonuclear process with energies around 2.45 MeV.

The measured width of the scattered peak  $\sim 45$ –70 ns is also individual for each discharge and is an upper estimate of the generation duration of the narrow beam of neutrons. The predominant process of elastic neutron scattering at an angle of about  $113^\circ$  (from the concrete ceiling toward the detectors), which allows the diagnosis of the neutron jet exiting along the PF axis, is elastic scattering on oxygen. The limiting energy of the beam neutrons is 3.1–3.7 MeV and has an individual value for each discharge. It is estimated based on the change in the neutron energy during elastic scattering on the nucleus of an oxygen atom by the appropriate angle and the time of the neutron flight of the initial energy of the distance from the neutron source to the scattering region (ceiling) and then (with the changed energy) to the detector.

The last column of the table shows the number of counts per 100 s (from/100 s) of the activation neutron counter (AC), which can be viewed as a neutron output monitor in the first approximation. AC (Ag in the moderator) was set at a distance of 6 m at an angle of  $90^\circ$  to the axis of the chamber. There is no connection between the monitor readings and the presence or absence of the  $n_{scat}$  peak on the oscillograms of the SD signals.

## 2. Modeling the SD signal when measuring plasma focus emission in a closed space

The simulation of the time dependence of the SD signal at a distance of 9 m from the source observed in the experiment was performed within the framework of the hypothesis of the presence of a neutron flux narrowly directed along the chamber axis in the radiation composition of the PF-chamber. For computational modeling of the registered detector signal, initial data close to those recorded in the experiment were chosen. The simulation considered a superposition of two independent neutron sources — 1) — generating neutrons in all directions and 2) — a narrowly focused neutron beam with a  $3^\circ$  angular divergence between the device axis and the cone shape.

For a  $Y_{all}$  source generating neutrons in all directions and forming a straight peak, an anisotropic distribution of neutron escape energy and angle, corresponding to the differential cross section of the DD reaction for neutron energy escaping at an angle of  $0^\circ$  —  $E_n(0^\circ) = 2.96$  MeV, at  $80^\circ$  —  $E_n(80^\circ) = 2.56$  MeV [11], energy of bombarding deuterons — 0.15 MeV. The time dependence of the neutron generation pulse shape was set close to a Gaussian with a half-height width of 80 ns and a step of 20 ns.

For a narrowly directed neutron beam  $Y_{nf}$  the beam neutron energy was assumed to be 3.5 MeV, and the beam angular divergence —  $3^\circ$  between the device axis and the cone shape. In the course of, the angular divergence was varied from  $3$  to  $15^\circ$  to estimate the effect of the size of the scattering region on the duration of the scattered peak. Beam generation in time was set uniformly in the interval 20 ns.

The result of the calculations is the light output from the scintillator, calculated with the light-output model described in [12], proportional to the detector output current and the voltage taken from the detector and recorded on the oscillogram.

Fig. 4 shows the results of model calculations for the source  $Y_{all}$  (dashed line) and the superposition of sources (solid line). The horizontal axis is time in nanoseconds, the vertical axis — the value in units (a.u.) proportional to the light produced in the scintillator by the radiation incident on the detector. The ratio of neutron yield in all directions  $Y_{all}$  to neutron yield in the narrow beam  $Y_{nf}$ , equal to  $Y_{all} : Y_{nf} = 1 : 0.2$ , was taken to superimpose the model calculations.

The solid line corresponds to the oscillogram in Fig. 2 — the peak  $\sim 600$ – $700$  ns corresponds to neutrons scattered in the interaction region of the neutron beam with the ceiling of the experimental hall. The dotted line corresponds to the oscillogram in Fig. 3 for the absence of the scattered neutron peak. Both the overall picture and the temporal position of the characteristic peaks of the calculated dependence correspond to the experimental oscillograms.

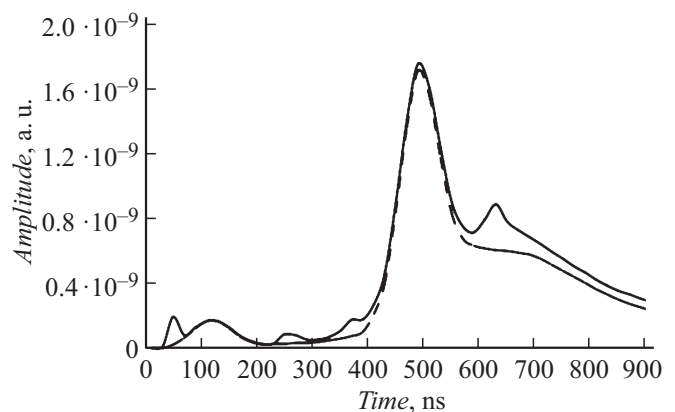


**Figure 4.** Calculated time dependence of the detector signal from sources  $Y_{all}$  (dashed line) and the superposition of sources  $Y_{all}$  and  $Y_{nf}$  (solid line,  $Y_{all} : Y_{nf} = 1 : 0.2$ ).

The ratio of the areas of the main and scattered peaks on the simulated time dependence of the scintillator light output (Fig. 4) is  $S_{dir} : S_{scat} = 24$ . In the experiment for the discharges presented in the table, where the peak of scattered neutrons is fixed (lines 1–5), this ratio varies from 11 to 48. Neutron yields in the experiments were as high as  $1.1 \cdot 10^{11}$  neutrons per discharge [7]. From this it is easy to estimate the narrow beam yield for these discharges — it is  $\sim 10^{10}$  of neutrons per discharge with noticeable variation from discharge to discharge. Recall that there is no correlation between the areas of the direct and scattered peaks (up to complete indistinguishability of the scattered peak), which means that the corresponding processes of the generation of these and other neutrons are independent.

The effect of angular divergence of the beam directed along the chamber axis on the width of the scattered neutron peak by increasing the size of the scattering region on the ceiling when the radiation cone angle is increased was investigated in calculations. For angles equal to  $3$  and  $5^\circ$  between the device axis and the cone formative, the calculated peak width agrees with experiment —  $40$ – $50$  ns, but for angles of  $10$  and  $15^\circ$  it noticeably exceeds (respectively  $90$  and  $140$  ns) the values recorded in the measurements (table, column  $t_{1/2,scat}$ ). The change in the shape of the time dependence of the beam generation from uniform in the 20 ns interval to a near-Gaussian with „halfwidth“ 60 ns also leads to an excess of the calculated width of the scattered peak (FWHM = 92 ns) over that fixed in the measurements.

From this we can conclude that the bulk of the narrow beam of neutrons for the discharges given in the table — (lines 1–5) is confined within  $\sim 3$ – $5^\circ$  between the device axis and the radiation cone formation, and the duration of its generation does not exceed several tens of nanoseconds.

It follows from the calculation results that the anisotropy of the angular distribution of the source, which is proportional to the differential cross section of the DD reac-

tion with maximum neutron energy  $E_n(0^\circ) \sim 2.96$  MeV, does not explain the presence of a distinct peak in the 600–700 ns interval in the experimental oscillograms. It is even more impossible to explain the presence of such a peak in the case of fusion neutron generation (2.5 MeV) with isotropic yield.

Modeling features of experimental oscillograms are not tied to the description of results in a particular discharge, but demonstrate and explain the only possible cause of the occurrence (formation) of the registered measurement results.

### 3. Discussion of results

The processing of experimental records and their Monte Carlo simulation allow us to conclude that a special type of non-thermal neutron fusion mechanism is realized in some discharges in the plasma focus chamber, namely, the generation of a neutron beam (flux) with an energy  $\sim 3.5$  MeV narrowly directed along the chamber axis, independent of other generation processes—accelerator according to the „beam–target“ and thermonuclear fusion models.

The integral yield of this beam can be a noticeable fraction compared to the integral yield due to other mechanisms of neutron generation in the PF. The duration of generation of a narrowly focused neutron beam is estimated to be several tens of nanoseconds. The angular divergence of the beam is estimated by  $\sim 3\text{--}5^\circ$ .

This is evidenced by:

- localization of the scattered neutron peak on the time scale for two detector distances from the source (6 and 9 m), corresponding to the span times to the detectors of neutrons elastically scattered from the room ceiling,
- ratio of the areas of the main and scattered peaks,
- duration of the scattered neutron peak,
- absence of correlation in the series of discharges between the area of the direct and scattered peaks up to the complete absence of the scattered peak.

The neutron energy of the  $\sim 3.5$  MeV beam indicates an undoubted connection between the mechanism of generation of narrow-directional radiation from the plasma focus and accelerated ions. The generation of a narrowly focused beam of DD neutrons is one type of accelerator mechanism for generating neutrons in plasma-focused devices. The anomalously high degree of anisotropy (from 3.3 to 6) of the neutron fluence in the experiments may be related to this process [1–3]. Finding out the details of the mechanism of this type of neutron generation is a subject for further research.

The AC (Ag in moderator) used in the experiments, as shown by the MC calculations, is insensitive to the contribution of narrow beam neutron generation to the total neutron yield. The Ag-monitor readings are practically unchanged for the model calculations, the results of which are shown in Fig. 4 — the variation of the indicator activation does not exceed 15%, which is significantly less

than the variation of the monitor readings from discharge to discharge.

It should be noted that the multicomponent mixture of elements of the concrete ceiling, the scattering from which was reproduced in the calculations, makes a detailed analysis difficult — it is rather a qualitative consideration with the highlighting of the characteristic features of the process. The possibility of accurate quantitative measurements opens up a special measurement method according to the patent [13], where a scatterer (e.g., graphite) with fixed dimensions, set in a certain way, provides scattering of the axial beam of DD neutrons only in an elastic process, and thereby simplifies obtaining quantitative results.

## 4. Prospects for studies of the parameters of narrowly focused neutron radiation generation

### 4.1. Positioning of activation detectors perpendicular to the chamber axis

Neutron generation in PFs is believed to be due to two main mechanisms — fusion and acceleration („beam–target“ model), with varying relative contributions depending on the design of the particular device and its mode of operation. The anisotropy of the yield and energy of the generated neutrons is associated with the acceleration mechanism of fusion. Determining the relative contribution of both mechanisms to the total generation of neutron radiation is very difficult both theoretically and experimentally. It is generally accepted that the contributions of these mechanisms are comparable (from 50 : 50 to 70 : 30). The question remains about the identity of the time parameters of these mechanisms of neutron generation.

The directional diagrams of fusion and acceleration neutrons are significantly different. The anisotropy coefficient for the  $Y_{all}$  source used in our calculations (see above) is  $\sim 2.5$ . Nevertheless, from the model calculations for the anisotropic source and for the isotropic source, it follows that the readings of the AC (Ag in the moderator) mounted perpendicular to the chamber axis for these options differ from the average by less than 10%.

It also follows from the calculations that the AC used in the experiments is virtually insensitive to the contribution of narrow beam neutron generation to the total neutron output. Its readings are practically unchanged for the model calculations, the results of which are shown in Fig. 4 — the change in activation of the indicator is less than 15%.

Both results are comparable with the measurement error and significantly less than the scatter of the AC detector readings (see table) from discharge to discharge.

A similar conclusion can be made for the threshold indicator based on the  $^{115}\text{In}(n, n')$  reaction, set at an angle of  $90^\circ$  to the axis of the chamber close to its outer surface.

Activation measurements with detectors (both threshold and nonthreshold) mounted perpendicular to the chamber axis do not answer the question of the relative contribution of different neutron generation mechanisms.

#### 4.2. Measuring the anisotropy coefficient with threshold indicators

Very sensitive to narrow beam generation, according to calculations, is the activation ratio of threshold indicators  $^{115}\text{In}(n, n')$  placed at angles  $0^\circ$  and  $90^\circ$  to the PF-camera axis. For our version of the measurements, the calculations show that the ratio of indicator readings  $0^\circ/90^\circ$  can differ by an order of magnitude, even if the contribution of narrow beam generation to the total process of neutron radiation generation is insignificant (a few percent). A similar conclusion can be drawn for the activation indicator based on the  $^9\text{Be}(n, a)$  reaction with a threshold of about 1 MeV.

In our experiments, the neutron energy of the narrow beam is estimated to be more than 3 MeV. Measurements by neutron radiation indicators with a threshold of  $> 3$  MeV can also provide useful information about the parameters of the beam exiting along the axis of the chamber.

An obvious advantage of the threshold activation neutron indicators is the significantly lower (compared to the Ag counter in the moderator) contribution of scattered radiation and insensitivity to X-ray and gamma radiation from the plasma focus and the environment.

#### 4.3. Oscillographic measurements of temporal generation parameters

The possibility to accurately quantify the characteristics of the narrow-directional radiation of DD-neutrons opens up a special measurement method according to the patent [13], where a scatterer (for example, graphite) with fixed dimensions, set in a certain way, provides scattering of the axial beam of DD-neutrons in an elastic process only and thus simplifies obtaining quantitative results. This reduces the number of measurement channels used — signals from neutron sources of different nature (fusion and accelerator-driven) are recorded on a single detector. Combined with the use of threshold activation indicators to measure the anisotropy, such a revision of the measurements will make it possible to unambiguously assess the quantitative characteristics of the narrow-directional neutron flux.

### Conclusion

The results of processing experimental time dependences of SD signals under conditions of measurements in a room of limited dimensions and modeling these time dependences by the Monte Carlo method indicate the presence in the plasma focus discharge of a special process of generating a neutron beam narrowly directed along the axis of the plasma focus device — the third type of generation of DD-neutrons,

complementing the two well-known processes — thermonuclear and the accelerator according to the „beam–target“. Generation of such a beam of DD-neutrons can be regarded as one of the types of gas pedal mechanism of neutron generation in plasma-focused devices.

Monte Carlo simulation of SD signal formation for specific experimental conditions allowed to reproduce the time pattern of signal dependence, coinciding with the corresponding features of the experimental oscillogram. The simulation considered a superposition of two independent neutron sources: 1) generating neutrons in all directions and 2) a narrowly focused neutron beam with an angular divergence of  $3^\circ$  between the device axis and the forming cone.

According to the results of processing experimental records and their Monte Carlo simulation, the parameters of the generated narrow beam of neutrons can be estimated as follows: the integral yield of the beam is comparable to the integral yield due to other mechanisms of neutron generation in the plasma focus chamber and is estimated in the considered measurements as up to  $\sim 10^{10}$  neutrons per discharge; the duration of narrow beam neutron generation does not exceed several dozen nanoseconds; the main part of the beam is enclosed in the angular interval  $\pm(3-5)^\circ$  from the axis of the plasma focus device.

In further research, it is recommended to use the patented method of making measurements with a localized scatterer.

### Funding

The work was performed within the framework of the state order of the Russian Federal Nuclear Center — All-Russian Research Institute of Experimental Physics (Contract H.2z.217.05.21.2107).

### Conflict of interest

The authors declare that they have no conflict of interest.

### References

- [1] F. Castillo-Mejía, M. Milanese, R. Moroso, J. Pouzo. *J. Phys. D: Appl. Phys.*, **30**, 1499 (1997).
- [2] M.V. Roshan, R.S. Rawat, A. Talebitaher, P. Lee, S.V. Springham. *Phys. Plasmas*, **16**, 053301 (2009). DOI: 10.1063/1.3133189
- [3] S.V. Springham, R. Verma, M.S.N. Zaw, R.S. Rawat, P. Lee, A. Talebitaher, J.H. Ang. *Nuclear Inst. Methods in Phys. Research, A* **988**, 164830 (2021).
- [4] V.E. Ablesimov, Yu.N. Dolin, O.V. Pashko, Z.S. Tsibikov. *Fizika Plazmy*, **36** (5), 436 (2010).
- [5] R. Niranjana, R.K. Rout, R. Srivastava, T.C. Kaushik, S.C. Gupta. *Rev. Scientific Instruments*, **87**, 033504 (2016). DOI: 10.1063/1.4942666
- [6] A.E. Dubinov, E.I. Fomicheva, L.A. Senilov. *Rev. Modern Plasma Physics*, **4**, 6 (2020). DOI: 10.1007/s41614-020-0041-1

- [7] V.E. Ablesimov, A.V. Andrianov, A.A. Bazanov, A.M. Glybin, Yu. V. Karpov, A.I. Kraev, S.S. Lomtev, V.N. Nudikov, S.V. Pak, N.I. Pozdov, S.M. Polyushko, A.F. Rybakov, A.N. Skobelev, A.N. Turov, A.Y. Fevralev. *PMTEF*, **1**, 94 (2015).
- [8] A.I. Veretennikov, K.N. Danilenko (coauthor). Diagnostic tools for single pulse radiation. *Collected Works of the NIIIT*. (IzdAT, M. 1999)
- [9] A.K. Zhitnik, E.N. Donskoy, S.P. Ognev, A.V. Gorbunov, A.N. Zalyalov, N.G. Ivanov, A.G. Malkin, V.I. Roslov, T.V. Semenova, A.N. Subbotin. *Voprosy atomnoy nauki i tekhniki. Ser. Mathematical Modeling of Physical Processes*, **1**, 17 (2011) .
- [10] V.E. Ablesimov, O.Yu. Pasharina. *Voprosy atomnoy nauki i tekhniki. Ser. Mathematical Modeling of Physical Processes*, **1**, 34 (2020).
- [11] H. Liskien, A.Paulsen. *Nucl. Data Tables*, **11**, 569 (1973).
- [12] A.E. Shmarov, V.I. Semenov. *Trudy RFYATS-VNIIEF*, **19** (1), 182 (2014).
- [13] V.E. Ablesimov. Method for measuring the angular radiation characteristics of a pulsed neutron source (Patent of the Russian Federation for the invention № 2738688. Invention Priority March 02, 2020)